Table 1 Optimum fiber directions

No. of layers	k	a/b	Fiber directions, deg α_1	α_2	α_3	α_4	α_5	α_6	Reduced critical stress, ϕ
3	0	1.0	45	45	45				22.000
4	0	1.0	45	45	45	45			22.000
6	0	0.5	0	0	0	0	0	0	42.171
6	0	0.8	38	38	38	38	38	38	23.154
6	0	1.0	45	45	45	45	45	45	22.000
6*	0	1.25	49.9	51.0	48.6	48.8	51.0	49.9	23.116
6	0	2.0	45	45	45	45	45	45	22.000
6*	0.5	0.5	7.9	3.8	22.1	0.5	7.4	12.3	37.024
6	0.5	1.0	45	45	45	45	45	45	14.667
6*	0.5	2.0	67.1	56.4	56.2	55.5	64.0	61.4	12.556
6	1.0	1.0	45	45	45	45	45	45	11.000
6*	1.0	2.0	71.6	68.1	77.5	61.2	71.1	74.1	8.051

not. Therefore, trials with several starting points are desirable.

Numerical Examples

Numerical calculations were made for laminated plates with three, four, and six layers. The plates considered have various aspect ratios and are under uniaxial or biaxial compression. Seven or eight different combinations of fiber directions are used to start the calculation. The computer code[6] developed by Powell was rearranged into the code written for the present problem.

The convergence limits for all the design variables were set equal to 0.1 deg, and the maximum step size multiplier[6] in single variable search was set equal to 10.0. The material consider is boron/epoxy.

$$E_1 = 2.11 \times 10^4 \text{ kg/mm}^2 \ (30 \times 10^6 \text{ psi})$$

$$E_2 = 2.11 \times 10^3 \text{ kg/mm}^2 \ (3 \times 10^6 \text{ psi})$$

$$\nu_{12} = 0.3, \ G_{12} = 7.03 \times 10^2 \text{ kg/mm}^2 \ (1 \times 10^6 \text{ psi})$$

The thickness of each layer is assumed to be 0.254 mm (0.01 in.). The buckling formula is a function of the half-waves in the x and y directions. Therefore, the number of half-waves in the x and y directions was varied from 1 to 10 and from 1 to 5, respectively, to get the buckling stress for the assigned fiber directions.

The numerical results for three- and four-layered plates with $a/b = 1$ and $k = 0$ showed that the results obtained do not depend on the starting values of fiber directions. To show the numerical convergence, an example is presented in Fig. 1. In this figure, the abscissa is the number of the iteration. Each iteration includes many function evaluations. The method was next applied to six-layered plates with various aspect ratios and load ratios k. A summary of all the numerical results is given in Table 1. In this table, asterisks show that the final results obtained depend on the starting values, and the values shown correspond to the highest critical buckling stress obtained among eight cases with different starting values. In these cases, the critical buckling stresses obtained are not much different from each other, but the fiber directions depend highly on the starting values. The fiber directions in the rows without an asterisk have no decimal, because almost all of the directions obtained for seven or eight cases are close to the values shown.

The computer used was IBM 360/67 and average cpu time to calculate eight cases for a six-layered plate under $k = 0$ was 158 s.

Acknowledgment

The author wishes to acknowledge the helpful advice of N. J. Hoff of Rensselaer Polytechnic Institute. This work was supported by NASA under Grant NGL-33-018-003.

References

[1] Housner, J. M. and Stein, M., "Numerical Analysis and Parametric Studies of the Buckling of Composite Orthotropic Compression and Shear Panels," NASA TN D-7996, Oct. 1975.

[2] Jones, R. M., *Mechanics of Composite Materials*, McGraw-Hill Book Co., Inc., New York, 1975, pp. 154-155.

[3] Whitney, J. M. and Leissa, A. W., "Analysis of Heterogeneous Anisotropic Plates," *Journal of Applied Mechanics*, Vol. 36, June 1969, pp. 261-266.

[4] Almroth, B. O., "Influence of Edge Conditions on the Stability of Axially Compressed Cylindrical Shells," *AIAA Journal*, Vol. 4, Jan. 1966, pp. 134-140.

[5] Powell, M.J.D., "An Efficient Method for Finding the Minimum of a Function of Several Variables without Calculating Derivatives," *Computer Journal*, Vol. 7, July 1964, pp. 155-162.

[6] Kuester, J. L. and Mize, J. H., *Optimization Techniques with Fortran*, McGraw-Hill Book Co., Inc., New York, 1973, pp. 331-343.

Flexural Vibration of Orthotropic Cylindrical Shells in a Fluid Medium

D.B. Muggeridge* and T.J. Buckley†
Memorial University of Newfoundland, St. John's, Newfoundland, Canada

Introduction

The problem of free vibration of a cylindrical shell has interested many investigators since the time of Rayleigh. In recent years this interest has continued in the area of composite shells, due to their increasing importance in aerospace and hydrospace applications.

The first experimental determination of natural frequencies of cylindrical shells was made by Arnold and Warburton[1]

Received Oct. 13, 1978; revision received March 26, 1979.

Index categories: Aeroelasticity and Hydroelasticity; Structural Composite Materials.

*Associate Professor, Faculty of Engineering and Applied Science.
†Project Engineer, formerly with Faculty of Engineering and Applied Science.

using freely supported steel cylinders. These shells were excited by an electromagnet and the natural frequencies were determined by noting maximum sound levels.

More recently, a number of other researchers have investigated the vibration characteristics of isotropic cylindrical shells with various boundary conditions. However, very few results exist for orthotropic or generally anisotropic shells. One of the few such sets of results are due to Karimbaer et al.,[2] who determined natural frequencies and mode shapes of glass-fiber reinforced plastic shells by mounting the test cylinders on top of a large shaker.

Several theoretical papers have considered the problem of vibration of orthotropic and anisotropic shells. Other theoretical papers have considered the vibration characteristics of isotropic shells that are filled with or surrounded by a fluid, and a few have concentrated on fluid-filled orthotropic shells.[3,4] It is these last papers that form the starting point of the present study.

Theory

The governing partial differential equations for free vibration of an orthotropic, circular cylindrical shell in an infinite, inviscid, and incompressible fluid may be found in Ref. 3. The solution of these equations for arbitrary boundary conditions is due to Dong.[5] A characteristic equation was obtained that was eighth order in a characteristic length and sixth order in the natural circular frequency. An iterative procedure was then used to obtain an explicit solution of the indicial equation, for the characteristic lengths. The system of clamped boundary conditions was then tested and if it was met, the correct natural frequency was found. Otherwise, a subsequent iteration was necessary.

Experimental Procedure

The experimental phase of the program involved the testing of a four-ply, glass-epoxy "Scotchply" type 1002 preimpregnated tape-wound cylinder. This shell was fabricated on a custom-made belt wrapper that utilized an aluminum mandrel. The ends of the shell were overwrapped with several circumferential layers prior to thermal curing under vacuum. The completed shell was then cast into aluminum end plates with epoxy. Material properties were taken from data supplied by Tennyson (Institute for Aerospace Studies, University of Toronto). These data on orthotropic in-plane material constants were obtained from identical test shells fabricated on the same type of belt wrapper. The characterization tests required three loading configurations: internal pressure, torsion, and compression. Foil strain gages were bonded in the axial, circumferential, and ±45 deg directions at midlength on the outer surface of the shell and the resultant data were used to compute the orthotropic material constants. Four coupons were cut from the shell to determine the filament weight content using a resin burn-off test. Rule of mixtures calculations were then made to compare with the measured orthotropic constants and reasonable agreement was obtained. A summary of geometric and material properties is contained in Table 1.

The shells were held between adjustable centers by their end plates inside an aluminum tank. Excitation was provided by a 44.5 N electrodynamic shaker which could be mechanically connected to various stations along the generator of the shell. Water could be introduced into the shell via holes in its end plates and the entire shell could be either partially or fully submerged by filling the tank.

The resonant frequencies of the shell were determined by point impedance measurements. A constant velocity, at the point of excitation, was maintained by feedback of the in-

Table 1 Shell geometric and material properties[a]

Lamina	Thickness, mm	Orientation, deg	Orthotropic constants
1 (inner)	0.283	+45	$E_{11} = 34.2$ GN/m^2
2	0.308	−45	$E_{22} = 10.4$ GN/m^2
3	0.319	−45	$G_{12} = 3.65$ GN/m^2
4 (outer)	0.321	+45	$\nu_{12} = 0.28$

[a] Radius/thickness = 85.54; length/radius = 7.50.

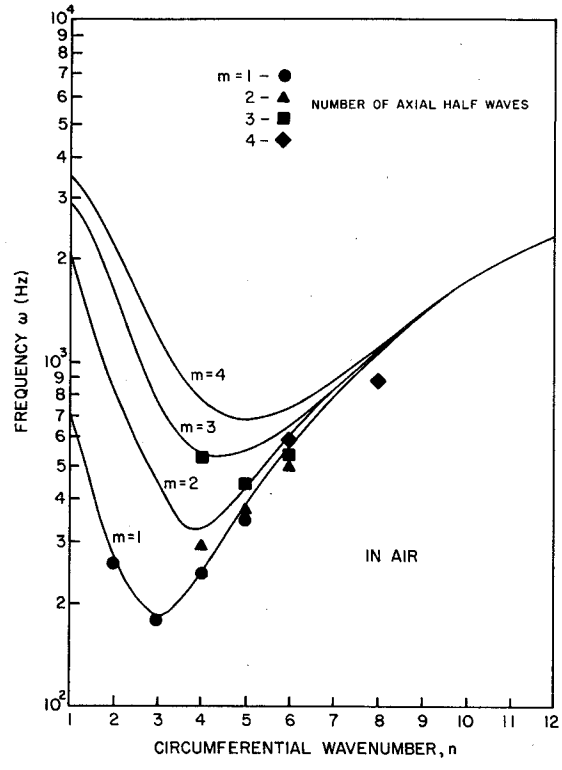

Fig. 1 Comparison of experimental results with theory for a shell in air.

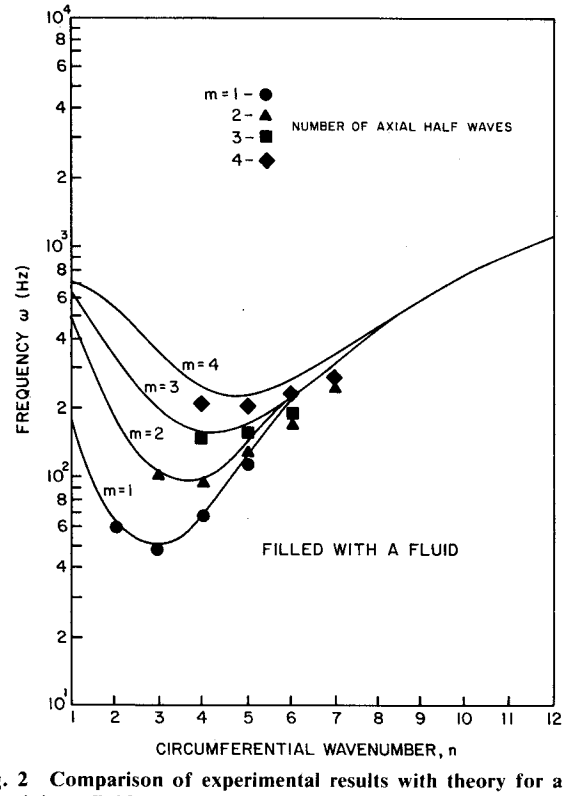

Fig. 2 Comparison of experimental results with theory for a shell containing a fluid.

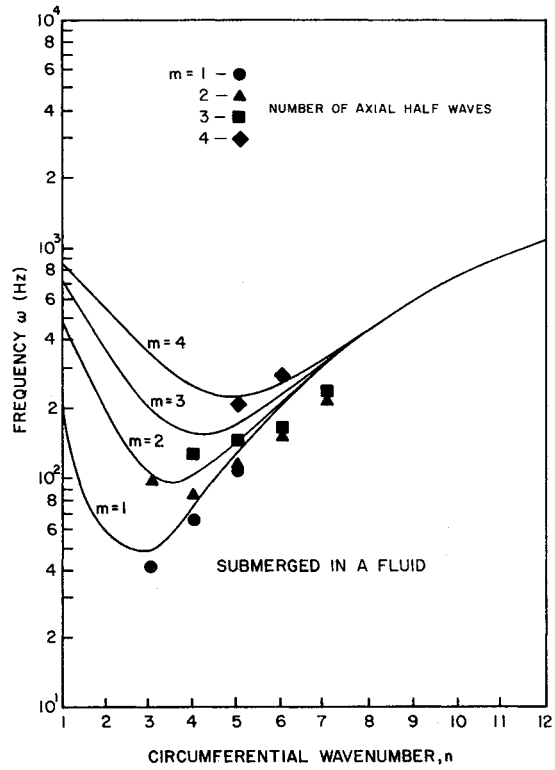

Fig. 3 Comparison of experimental results with theory for a shell immersed in a fluid.

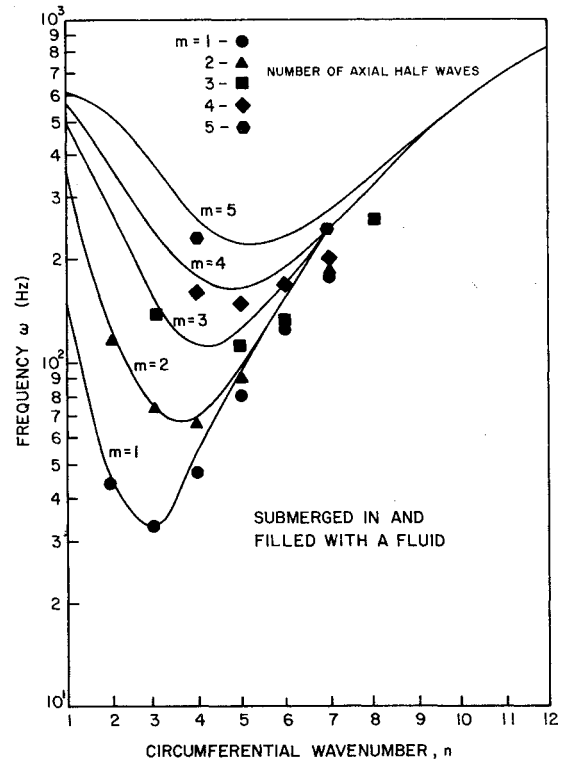

Fig. 4 Comparison of experimental results with theory for a fluid filled shell immersed in a fluid.

tegrated acceleration signal from the impedance head. A spring loaded accelerometer probe was used to identify the modes of vibration. This probe could readily transverse in the axial and circumferential directions via a motorized lead screw and chain driven sprocket arrangement. Position of the probe was obtained from potentiometers.

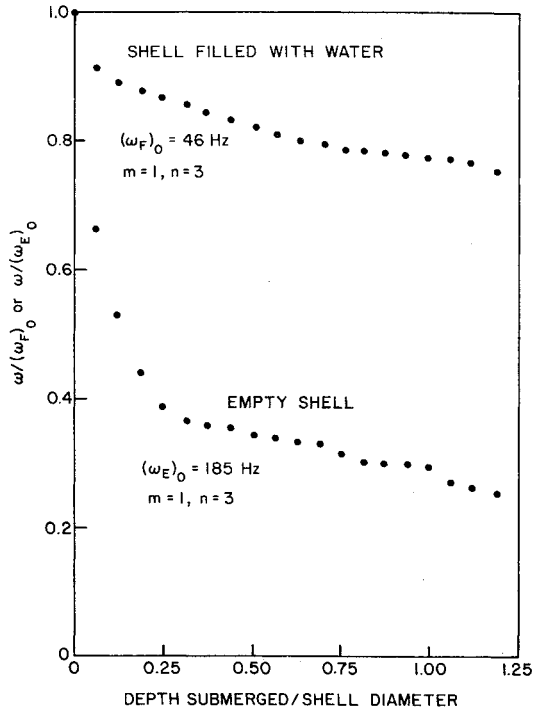

Fig. 5 The effect of submergence on the natural frequency of empty and fluid filled shells.

Experimental Results and Discussion

A comparison of experimental results with theory is shown in Figs. 1-4 for the four cases investigated; namely, a shell in air, a shell containing a fluid, a shell immersed in a fluid, and a fluid filled shell immersed in a fluid. The natural frequency of flexural vibration of the shell immersed in, or filled with, a fluid is less than a quarter of that of the corresponding natural frequency of the shell in air. Results from a shell immersed in a fluid and a shell containing a fluid are almost identical. However, the immersed shell had slightly lower natural frequencies. A fluid filled shell when submerged exhibits lower natural frequencies than any of the other test cases investigated. The theory also predicts a further decrease in natural frequency as the density of the fluid is increased. A greater number of natural frequencies and mode shapes were detected for the fluid interaction cases than that of the shell in air. Generally good agreement between theory and experiment was noted for the natural frequencies and mode shapes that were excited and detected.

Weingarten et al.[5] showed theoretically that the natural frequency of a partially submerged cylindrical shell decreases rapidly until a point where the cylinder is approximately one quarter submerged. Thereafter the fundamental frequency is relatively insensitive to further submergence. This conclusion has been verified experimentally (see Fig. 5) where the lowest natural frequency of vibration of an empty shell was observed to decrease rapidly with initial submergence followed by a gradual decrease due to increasing hydrostatic pressure. The fluid filled shell behaved much the same except that there was a more gradual decrease in frequency.

Conclusions

The flexural mode frequencies decrease to a minimum and then increase as the circumferential mode number is decreased. It is clear that for any particular axial wave number, the natural frequency is substantially decreased due to the presence of the fluid.

Acknowledgments

W.N. Dong was responsible for the initial theoretical phase of this work[3] and L. Zeidler obtained the data that were

presented as Fig. 5. The authors gratefully acknowledge the finanical support of the National Research Council of Canada (Grant No. A8668).

References

[1] Arnold, R.N. and Warburton, G.B., "Flexural Vibration of the Walls of Thin Cylindrical Shells Having Freely Supported Ends," *Proceedings of the Royal Society (London), Series A*, Vol. 197, June 1949, pp. 238-256.

[2] Karimbaer, T.D., Koroler, V.P., and Epanov, V.G., "Experimental Investigation of Frequencies and Forms of Natural Vibration of Glass-Fibre Reinforced Plastic Shells," *Problemy Prochnosti*, Vol. 6, May 1974, pp. 31-33 (in Russian).

[3] Dong, W.N. and Muggeridge, D.B., "Vibration Characteristics of Reinforced Plastic Pipe in a Fluid Medium," IEEE Ocean International Conference, Halifax, Nova Scotia, Aug. 1974, pp. 418-424.

[4] Jain, R.K., "Vibration of Fluid-Filled, Orthotropic Cylindrical Shells," *Journal of Sound and Vibration*, Vol. 37, No. 3, 1974, pp. 379-388.

[5] Weingarten, V.I., Masri, S.F., and Lashkari, M., "Free Vibration of a Partially Submerged Cylindrical Shell," *Hydromechanically Loaded Shells, Proceedings of the 1971 Symposium of the International Association for Shell Structures*, Honolulu, University Press of Hawaii, 1973, pp. 591-601.

Screening of Liquids for Thermocapillary Bubble Movement

William R. Wilcox* and R. Shankar Subramanian†
Clarkson College of Technology, Potsdam, N.Y.
John M. Papazian‡
Grumman Aerospace Corporation, Bethpage, N.Y.
and
Harry D. Smith§ and Douglas M. Mattox¶
Westinghouse R&D Center, Pittsburgh, Pa.

Nomenclature

C_p = heat capacity of melt, kJ/kg·K
D_b = diameter of bubble, m
Gr = Grashof number, $g\alpha\beta h^4/\nu^2$
h = thickness of layer of liquid, m
k = thermal conductivity of liquid, W/m·K
ℓ = length of layer of liquid, from hot wall to cold wall, m
Pr = Prandtl number, ν/κ
q = rate of heat loss from cell, W/m^2
Ra_h = horizontal Rayleigh number, $\alpha\beta g h^4/\kappa\nu$
T = temperature at point in liquid, K
V = velocity of movement of melt due to buoyancy and surface tension, m/s
V_b = velocity of movement of bubble under influence of ΔT, m/s
y = vertical distance from bottom of liquid to any point, m
α = coefficient of thermal expansion of liquid, $(\partial\ \ell n\rho/\partial T)$, K^{-1}
β = longitudinal temperature gradient, K/m
γ = surface tension between liquid and gas, N/m
κ = thermal diffusivity, $k/\rho C_p$, m^2/s
μ = dynamic viscosity, kg/m·s
ν = kinematic viscosity, m^2/s
ρ = density of melt, kg/m^3

Received Sept. 1, 1978, revision received March 26, 1979.

Index categories: Thermophysical Properties of Matter; Hydrodynamics; Materials, Properties of.

*Professor and Chairman, Dept. of Chemical Engineering.
†Associate Professor, Dept. of Chemical Engineering. Member AIAA.
‡Senior Research Scientist, Materials and Structural Mechanics, Research Dept.
§Senior Scientist, Ceramic Systems.
¶Manager, Ceramic Systems.

THE objective of this work was to develop a technique for ascertaining thermocapillary movement of gas bubbles in a liquid. Gas bubbles have been found to be incorporated much more often in space-processed materials than in those processed on Earth.[1-6] The behavior of gas bubbles is expected to be especially important in containerless processing of glasses in orbit. Although buoyancy would no longer provide appreciable migration rates, gas bubbles are predicted to move in a temperature gradient due to the dependence of surface tension on temperature, with a velocity equal to[7,8]

$$V_b = -\frac{D_b}{4\mu}\frac{\partial\gamma}{\partial T}\nabla T \tag{1}$$

Thus one might expect that if $\partial\gamma/\partial T \neq 0$, a bubble in a liquid would always move in an imposed temperature gradient. However, surfactants may prevent the bubble from moving, as apparently happened in SPAR experiments on molten CBr_4.[1,9] Volatile constituents may also cause movement in the opposite direction.[10-12]

For flight experiments, some method is required to pretest the qualitative behavior of a gas bubble. We have chosen to use horizontal tubes or layers. Unfortunately, experiments done on Earth are complicated not only by the buoyant rise of the bubble but also by natural convection of the liquid itself. With a bubble in a tube or sheet, the prime concern is that any bulk movement of the liquid be much slower than the expected bubble movement. Fortunately there are existing theoretical results on similar systems, namely flat sheets of liquid with vertical end walls at different temperatures. We expect these to be approximtely true for our experimental arrangements, and Eq. (1) to provide an order-of-magnitude estimate for thermocapillary bubble movement rates in a horizontal channel or tube.

In the derivation of Eq. (1), it was assumed that steady-state conditions are valid, that the properties are constant, that there are no interactions with system boundaries or other bubbles, and that the liquid is pure.[7] Since in real situations these conditions are not satisfied, we seek here only semiquantitative tests of the usefulness of proposed experimental techniques.

Theory

It may be shown that the bubble always moves slower than the liquid if the upper surface is free.[13] Thus the liquid film must be enclosed on all sides. At the upper and lower horizontal surfaces, two types of boundary conditions on the temperature field are typically used to represent limiting cases. In one case, the boundaries are assumed to be insulated so that the normal heat flux through them is set equal to zero. In the other extreme, the temperature field is prescribed as being linear from one end of the channel to the other. This latter case is commonly referred to as that of "conducting" boundaries. In both cases, the parallel flow velocity field in the liquid film in a region away from the end walls (for a constant axial temperature gradient β) is given by[14-17]:

$$\frac{V\nu}{\alpha\beta g h^3} = \frac{(y/h)^3}{6} - \frac{(y/h)^2}{4} + \frac{y/h}{12} \tag{2}$$